

Mean-Field Analysis of Electric Field Effect on Charge Orders in Organic Conductors

Emi YUKAWA* and Masao OGATA

*Department of Physics, University of Tokyo
Hongo, Bunkyo-ku, Tokyo, 113-0033 JAPAN*

In order to investigate charge ordering phenomena under electric field, static nonequilibrium Hartree approximation (SNHA) method is formulated on the basis of the nonequilibrium Green's functions introduced by Keldysh. By applying the SNHA to the 3/4-filling extended Hubbard model on anisotropic triangular lattice, we study the stabilities and amplitudes of 3-fold and horizontal charge orders in θ and θ_d -(BEDT-TTF)₂X salts under the electric field. The obtained results show that the electric field stabilizes the 3-fold state in comparison to the horizontal state. The amplitude of the 3-fold state tends to decrease by the field, whereas that of the horizontal state does not change.

KEYWORDS: charge order, anisotropic triangular lattice, organic conductor, static nonequilibrium condition, Hartree approximation, nonequilibrium Green's function

One of the families of organic crystals, (BEDT-TTF)₂X (in short (ET)₂X), has quasi-two-dimensional nature. Its donors, BEDT-TTF (ET) molecules, and acceptors, Xs, form monolayers respectively, and they are stacked layer by layer. Spatial arrangements of ET molecules can be controlled by the anion molecules and hydrostatic pressure.¹ Among the different polytypes, ET layers in θ and θ_d -type crystals, which are focused on in this paper, form 3/4-filling anisotropic triangular lattices: the former is metallic and has no dimerization, whereas the latter is insulating and dimerized.

When the acceptor, X, is RbM'(SCN)₄ (M' = Co, Zn), (ET)₂X is a metallic θ -type material at room temperature. When this Rb salt is cooled slowly (slow-cooling condition), it undergoes a structural phase transition from θ type to θ_d at about 190K ($\equiv T_{\text{MI}}$), and becomes insulator.¹⁻³ Accompanying this transition, the electronic state also changes: above T_{MI} , a metallic short-range charge order (CO) characterized by a diffuse rod, $\mathbf{q} = (1/3, k, 1/4)$, is observed in X-ray measurements,⁴ while below T_{MI} , an insulating long-range CO characterized by a diffuse rod, $\mathbf{q} = (0, k, 1/2) \equiv \mathbf{q}_1$, is observed in NMR, X-ray, Raman scattering, and optical conductivity experiments.⁴⁻¹² The latter CO is called the horizontal CO, which has two-fold periodicity in real space.

On the other hand, when X is CsM'(SCN)₄ (M' = Co, Zn), the crystal remains θ type down to low temperature and no phase transition is observed.¹ Above 20K, it is metallic and a short-range 3-fold diffuse rod, $\mathbf{q} = (2/3, k, 1/3) \equiv \mathbf{q}_2$, is observed. At about $T = 20\text{K}$, the resistance starts to increase by 10^{4-6} times accompanied by an appearance of the short-range diffuse rod at $\mathbf{q} = \mathbf{q}_1$, which coexists with \mathbf{q}_2 .^{13,14} The wave number, \mathbf{q}_1 , is same as that observed in Rb salts below T_{MI} i.e., the horizontal CO. Since the horizontal CO will be accompanied by the θ_d type lattice structure, Cs salts are supposed to be in a super-cooled glass state consisting of inhomogeneous mixture of θ and θ_d -type lattice structures below 20K.^{5,15}

Recently, surprising current-voltage (I - V) characteristics are observed in Cs salts below 20K, where the short-range 3-fold and the horizontal CO coexist: a gigantic nonlinear conductivity^{16,17} and a thyristor like I - V characteristic.¹⁸ Furthermore, the X-ray measurements under a constant current below 5K show that the intensity of the horizontal diffuse rod decreases whereas that of the 3-fold remains. Therefore, the observed anomalous I - V characteristics are assumed to be due to the different dependences of CO state on the electric field or current. In Rb salts, under a rapid-cooling condition, the same phenomena as Cs salts have been observed.¹⁸

The main purpose of this paper is to understand these phenomena using an extended Hubbard model which is a canonical model describing charge ordered organic conductors. The preceding theoretical researches about charge ordering phenomena are often focused on stability and phase diagram under equilibrium condition.²⁰⁻²⁵ In this paper, we formulate static nonequilibrium Hartree approximation (SNHA) using Green's functions introduced by Keldysh.²⁶ In this method, the free energy in the presence of static electric field can be calculated. The I - V characteristic is also investigated. We will show that the electric field stabilizes the 3-fold CO when the horizontal and 3-fold states are quasi degenerate. This may explain the X-ray measurements under a constant current.

The model for the calculations is based on the following three hypotheses. (1) All calculations are carried out in the θ or θ_d -type crystal, although Cs salts may have a glass state consisting of the 3-fold state with the θ -type lattice and the horizontal state with the θ_d -type lattice structure. (2) The metallic state under the electric field is assumed to be the 3-fold state in the θ_d -type crystal in order to compare the energies, although experimentally, the crystal structure transforms into a new structure under the electric field, which is slightly different both from the θ and θ_d -type. (3) We compare the energies of the 3-fold and horizontal state calculated in the uniform states. This means that the boundary ener-

* E-mail address: yukawa@hosi.phys.s.u-tokyo.ac.jp

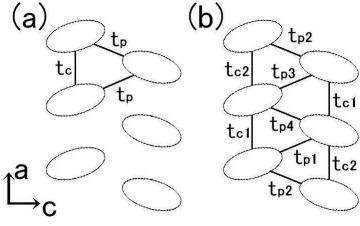


Fig. 1. Crystal structure and transfer integrals of (a) θ and (b) θ_d -(ET) $_2X$ in a donor layer.

Table I. Transfer integrals of θ_d -(ET) $_2$ RbZn(SCN) $_4$ at 90K calculated by the extended Hückel method.⁴

Transfer integral	θ_d -(ET) $_2$ RbZn(SCN) $_4$					
	c1	c2	p1	p2	p3	p4
($\times 10^{-2}$ eV)	1.5	5.2	16.9	-6.5	2.2	-12.3

gies between the metallic and the insulating regions are neglected.

Our Hamiltonian is written as the following extended Hubbard model:

$$H = \sum_{\langle x,y \rangle_{n.n.}, \sigma} (t_{xy} c_{x\sigma}^\dagger c_{y\sigma} + h.c.) + U \sum_x n_{x\uparrow} n_{x\downarrow} + \sum_{\langle x,y \rangle_{n.n.}} V_{xy} n_x n_y, \quad (1)$$

where t_{xy} is the transfer integral between sites, x and y , and U and V_{xy} are on-site and nearest-neighbor Coulomb repulsion, respectively. The summation, $\sum_{\langle x,y \rangle_{n.n.}}$, is over the pairs of nearest-neighbor sites. The operators, $c_{x\sigma}^\dagger$ ($c_{x\sigma}$) and $n_{x\sigma}$ represent a creation (an annihilation) and a number operator at site, x , with spin, σ . Throughout our calculations, U and the ratio V_c/U , are fixed at $U = 0.7$ eV and $V_c/U = 0.3$, respectively, which are typical values for organic conductors. The transfer integrals, t_{xy} , are $t_c = 4.3$ meV and $t_p = 11.3$ meV for the θ -type crystal as shown in Fig. 1. (a), and those for the θ_d -type crystal are given in Fig. 1. (b) and Table I.

When we apply the Hartree approximation, the Hamiltonian, H , is transformed into two parts, H_{MF} and a constant term. The former is bilinear in the electron operators. Taking twelve molecular sites as a unit cell, H_{MF} can be diagonalized in momentum space as,

$$H_{MF} = \sum_{\mathbf{k}\alpha\sigma} \tilde{c}_{\mathbf{k}\alpha\sigma}^\dagger \varepsilon_{\mathbf{k}\alpha\sigma} \tilde{c}_{\mathbf{k}\alpha\sigma}. \quad (2)$$

Here a new annihilation (creation) operator is written as $\tilde{c}_{\mathbf{k}\alpha\sigma} \equiv \sum_\beta u_{\mathbf{k}\beta\alpha}^* c_{\mathbf{k}\beta\sigma}$, where α and β represent the band index and the site number in a unit cell, and $u_{\mathbf{k}\beta\alpha}$ and $\varepsilon_{\mathbf{k}\alpha}$ are the eigenvector and the eigenvalue of H_{MF} , respectively. In this paper, a unit cell includes 12 molecules in order that both 3-fold and horizontal CO are fit in the unit cell. On the other hand, when we study the θ -type crystal, a unit cell with 3 molecules is used, because the θ -type crystal has no solution of the horizontal CO in the realistic parameter region.

In the SNHA method that we formulate, observables and self-consistent equations can be derived in terms of

the Green's functions introduced by Keldysh.²⁶ Here, we use the following Green's functions, so-called the *lesser* and *greater* Green's functions in the real space:

$$\begin{cases} G_{xy\sigma}^<(\tau, T) = i \langle \tilde{c}_{y\sigma}^\dagger(t') \tilde{c}_{x\sigma}(t) \rangle \\ G_{xy\sigma}^>(\tau, T) = -i \langle \tilde{c}_{x\sigma}(t) \tilde{c}_{y\sigma}^\dagger(t') \rangle, \end{cases} \quad (3)$$

with $\tau \equiv t - t'$ and $T = \frac{1}{2}(t + t')$, where the dependence of G on T can be ignored. In these definitions, $\tilde{c}_{x\sigma}(t)$ ($\tilde{c}_{x\sigma}^\dagger(t)$) is the annihilation (creation) operator of \tilde{H}_{MF} , which also includes the electric field term, $-en_x(t)\mathbf{x} \cdot \mathbf{E}$, and the impurity scattering term, both of which are bilinear. In terms of the *lesser* Green's function in Eq. (3), $\langle \tilde{H}_{MF} \rangle$ can be obtained as,

$$\begin{aligned} \langle \tilde{H}_{MF} \rangle &= \lim_{\eta \rightarrow 0^+} \lim_{y \rightarrow x} \sum_{x\sigma} \left[\frac{d}{d\tau} G_{xy\sigma}^<(\tau) \right]_{\tau=-\eta} \\ &= -i \lim_{\eta \rightarrow 0} \sum_{\mathbf{k}\alpha\sigma} \int \frac{d\omega}{2\pi} \omega e^{i\omega\eta} G_{\alpha\sigma}^<(\mathbf{k}, \omega), \end{aligned} \quad (4)$$

where $G_{\alpha\sigma}^<(\mathbf{k}, \omega)$ is the Fourier transform of $G_{xy\sigma}^<(\tau)$.

Then, according to the theory of quantum kinetic equation based on the Keldysh's method,²⁷ the *lesser* Green's function, $G^{<(1)}(\mathbf{k}, \omega)$ in the first order of $|\mathbf{E}|$ can be obtained as:

$$G^{<(1)}(\mathbf{k}, \omega) \sim ia(\mathbf{k}, \omega) \{n_F(\omega) - \Delta_{\mathbf{k}} n'_F(\omega)\}, \quad (5)$$

where $n_F(\omega)$ represents the Fermi distribution function. In (5), $a(\mathbf{k}, \omega)$ and $\Delta_{\mathbf{k}}$ are,

$$a(\mathbf{k}, \omega) = \frac{\gamma}{(\omega - \varepsilon_{\mathbf{k}\alpha\sigma})^2 + (\gamma/2)^2} \quad (6)$$

$$\Delta_{\mathbf{k}} = e\mathbf{E} \cdot \frac{\hbar^2 \mathbf{k}}{m \gamma}, \quad (7)$$

where the effective electron mass, m , in (ET) $_2X$ is assumed to be the free electron mass. In this formulation,²⁷ the relaxation rate, γ , naturally appears in $a(\mathbf{k}, \omega)$ and $\Delta_{\mathbf{k}}$ due to the presence of impurity scattering. In our calculation, the relaxation time, $\tau = \hbar/\gamma$ is fixed at 10^{-8} s in order to reproduce the resistivity.

We have extended the calculation for $G^{<(2)}(\mathbf{k}, \omega)$ up to the second order with respect to $|\mathbf{E}|$. After some straightforward manipulations, we obtain,

$$G_{\alpha\sigma}^{<(2)}(\mathbf{k}, \omega) \sim ia(\mathbf{k}, \omega) \{n_F(\omega) - \Delta_{\mathbf{k}} n'_F(\omega) + \Delta_{\mathbf{k}}^2 n''_F(\omega)\}, \quad (8)$$

which we approximate into the following expression:

$$G_{\alpha\sigma}^{<}(\mathbf{k}, \omega) \sim ia(\mathbf{k}, \omega) n_F(\omega - \Delta_{\mathbf{k}}). \quad (9)$$

Details of calculations will be published elsewhere. Since γ ($\sim 10^{-7}$ eV), is negligible compared to $k_B T$ ($\leq 10^{-3}$ eV), we approximate $a(\mathbf{k}, \omega)$ with delta function, $2\pi\delta(\omega - \varepsilon_{\mathbf{k}\alpha\sigma})$. With use of the *lesser* Green's function in (9), $\langle \tilde{H}_{MF} \rangle$ becomes,

$$\langle \tilde{H}_{MF} \rangle = \sum_{\mathbf{k}\alpha\sigma} \varepsilon_{\mathbf{k}\alpha\sigma} n_F(\omega - \Delta_{\mathbf{k}}). \quad (10)$$

In the same way, the self-consistent equations and expectation value of free energy and current are obtained in terms of $G_{\alpha\sigma}^{<}(\mathbf{k}, \omega)$.

Figure 2 shows the obtained ground state energies of horizontal and 3-fold CO in the θ_d type crystal for the

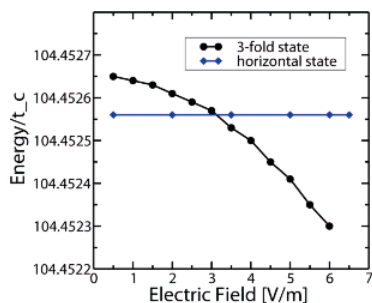


Fig. 2. Electric field dependence of the ground state energies at $V_p/V_c = 0.9$. The 3-fold CO state is stabilized by the electric field and it has a lower energy than the horizontal state for $|\mathbf{E}_c| > 3.2\text{V/m}$

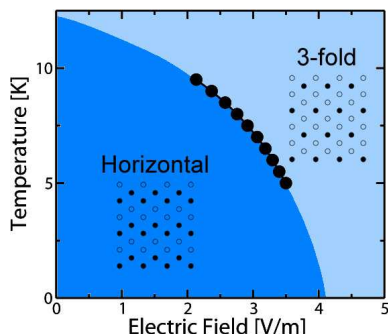


Fig. 3. The phase diagram against the temperature and the electric field. The small solid and open circles in each region represent the charge distribution of each CO.

case with $V_p/V_c = 0.9$. If the electric field is applied more than the critical field, E_c , the 3-fold state is stabilized in comparison to the horizontal state. We also calculated the ground state energies for $0.8 \leq V_p/V_c \leq 1.0$. When V_p/V_c is larger, the 3-fold CO state is more stable than the horizontal CO state.

Next, we calculate the free energies of two CO states at finite temperature, T , ranged from 5K to 10K. The anisotropy, V_p/V_c , is fixed at 0.89998 so that the energetic competition between the 3-fold and horizontal states is clearly seen. Figure 3 shows the critical electric field for various temperatures, which gives a phase diagram. As T increases, the 3-fold state is stabilized. Note that the free energy comparison is carried out in the θ_d -type structure, although experimentally the metallic 3-fold state is in the θ -type structure. In order to check the differences between the 3-fold state in θ and θ_d -type structure, we have studied the free energy of the 3-fold state in the θ -type, and found that the electric-field dependences are similar quantitatively. Therefore, if we compare the energies between the 3-fold state in the θ -type, we expect to obtain the same phase diagram as in Fig. 3.

We have also investigated the amplitude of the horizontal and 3-fold CO as a function of the electric field (not shown here). In this case we studied that the CO in the θ -type crystal instead of θ_d type, because the 3-fold CO in the θ_d type has the horizontal modulation. The

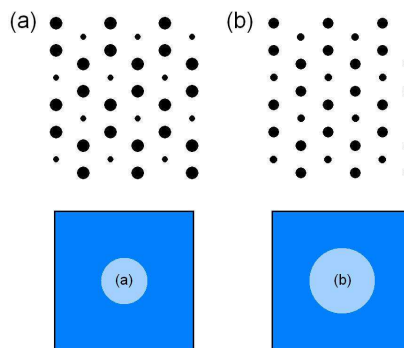


Fig. 4. Intensity, I , of a diffuse rod, \mathbf{q} , reflects both intensity (upper panels) and area of charge modulation (lower panels).

obtained results show that the electric field dependence of the amplitude of the 3-fold CO is $I = -aE^2 + 1.0$, with $a = 1.03 \times 10^{-6}$ at $T = 9.5\text{K}$. The more the electric field is applied, the weaker the intensity becomes. If the electric field is about 500V/m, where nonlinear conductivity is experimentally observed, we can expect 26% reduction of the amplitude, although our formulation can not be applied in such a strong field. On the other hand, the amplitude of the horizontal CO does not change by the electric field.

These results suggest that the electric field stabilizes the 3-fold CO but decrease its amplitude. We expect that the experimentally observed intensity of the diffuse rod, \mathbf{q}_2 , is affected by these two effects. Let us assume two cases as shown in Fig. 4. In (a), the amplitude of the 3-fold CO is twice stronger than that in (b). However, its area is half of that of (b). If one measures the X-ray diffraction in these two cases, one may observe diffuse rods with roughly the same intensity. Although it is necessary to consider the domain size and the boundary energies, it is possible that the total intensity of the 3-fold CO state does not change under the electric field, while that of the horizontal state decreases. If this is the case, the present calculation explains the tendency of what are observed in the X-ray measurements by Sawano et al.¹⁶

Finally, we would discuss the validity of the SNHA method. In the region of $|\mathbf{E}| < 1.0\text{V/m}$, the shift $\Delta_{\mathbf{k}}$ in the nonequilibrium Green's function in Eq. (7) is about $0.01t_c$, which is about 1/100 of the band gap of θ_d -(ET)₂X obtained in the tight-binding approximation. Although $\Delta_{\mathbf{k}}$ is small, there is an error in the replacement of $G^{<(2)}(\mathbf{k}, \omega)$ in (8) into $G^<(\mathbf{k}, \omega)$ in (9). This error can be estimated by,

$$\delta = \left| \frac{G^{<(2)}(\mathbf{k}, \mu) - G^<(\mathbf{k}, \mu)}{G^{<(2)}(\mathbf{k}, \mu)} \right|, \quad (11)$$

which is about 10^{-3} for $|\mathbf{E}| < 1.0\text{V/m}$. However, when $|\mathbf{E}|$ is larger than 1.0V/m, the error exceeds 0.3, since $\beta\Delta_{\mathbf{k}}$ appearing in $n_F(\omega - \Delta_{\mathbf{k}})$ becomes close to 1 at the low temperature (5K, for example). This means that in the higher electric fields, the error becomes larger, and higher order correlations in (8) become necessary. This is the reason why we only applied the SNHA for $|\mathbf{E}| < 6.0\text{V/m}$ in Fig. 2 and Fig. 3. To deal with the

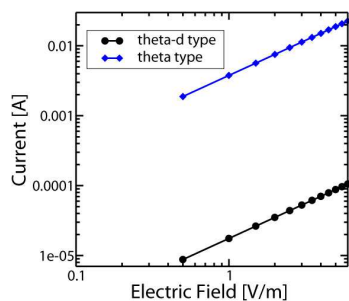


Fig. 5. I - V characteristics of 3-fold CO in θ and θ_d type crystals show linear conductivity.

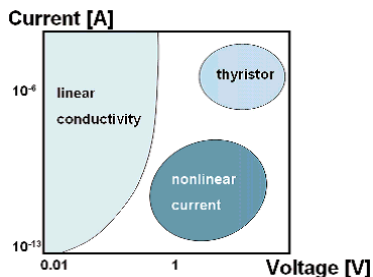


Fig. 6. Three parameter regions give linear conductivity, nonlinear conductivity, and thyristor-like characteristic, respectively.

higher electric fields, further improvements are necessary.

When we calculate the I - V characteristics in the present formalism, we obtain the linear conductivity as shown in Fig. 5. This is reasonable because the region that we study corresponds to the region where the linear conductivity is observed experimentally. The parameter regions are shown in Fig. 6 schematically. The present calculation corresponds to the left-hand side of this diagram. In this linear-conductivity region, the calculated resistivities of $\mathcal{O}(10^{-1})\Omega\text{cm}$ in the θ_d -type crystal are consistent with the measured resistivities of Rb salts of BEDT-TTF at about 200K. The calculated resistivities in the 3-fold CO of $\mathcal{O}(10^{-3})\Omega\text{cm}$ in the θ -type are 1/10 of the measured resistivities of Cs salts at about 200K.

In summary, we formulate the static nonequilibrium Hartree approximation (SNHA) method based on Keldysh's Green's functions in order to calculate the observables under the constant electric field. By applying this method to the 3/4-filled extended Hubbard model, we study the ground state energy with respect to anisotropy, V_p/V_c , the free energy at various temperatures, charge disproportion in a unit cell, and I - V characteristics. The results show that the electric field stabilizes the 3-fold state in comparison to the horizontal state. The charge amplitude of the 3-fold CO is decreased by the applied field, while the horizontal CO state is not affected. We speculate that these results explain the X-ray measurement in θ -(ET) $_2$ X at low temperature, in which the diffuse rod, \mathbf{q}_1 , has tendency to disappear, whereas \mathbf{q}_2 remains. The I - V characteristics for $|\mathbf{E}| < 6.0\text{V/m}$ is almost consistent with the experiments.

Since the SNHA method cannot be applied to higher electric field, we did not discuss the gigantic nonlinear conductivity and thyristor-like conductivity observed experimentally. Although further improvements in the SNHA method are necessary to deal with the high-field problems, the present method predicts tendency of behaviors of CO states under the static electric field.

Acknowledgment

We are grateful to professors H. Mori, I. Terasaki, and T. Nakamura for their fruitful advices. The present work is financially supported by Grands-in-Aid for Scientific Research on Priority Areas from MEXT, Japan.

- 1) H. Mori, S. Tanaka, T. Mori: Phys. Rev. B **57** (1998) 12023.
- 2) R. Chiba, K. Hiraki, T. Takahashi, H. M. Yamamoto, and T. Nakamura: Phys. Rev. Lett. **93** (2004) 216405.
- 3) K. Inagaki, I. Terasaki, and H. Mori: Physica B **329** (2003) 1162.
- 4) M. Watanabe, Y. Noda, Y. Nogami, and H. Mori: J. Phys. Soc. Jpn. **73** (2004) 116; *ibid* **74** (2005) 2011.
- 5) T. Nakamura, W. Minagawa, R. Kinami, Y. Konishi, and T. Takahashi: Synth. Met. **103** (1999) 1898.
- 6) K. Miyagawa, A. Kawamoto, and K. Kanoda: Phys. Rev. B **62** (2000) R7679.
- 7) R. Chiba, H. Yamamoto, K. Hiraki, T. Nakamura, and T. Takahashi: Synth. Met. **120** (2001) 919.
- 8) K. Yamamoto, K. Yakushi, K. Miyagawa, K. Kanoda, and A. Kawamoto: Phys. Rev. B **65** (2001) 085110.
- 9) H. Tajima, S. Kyoden, H. Mori, and S. Tanaka: Phys. Rev. B **62** (2000) 9378.
- 10) N. L. Wang, H. Mori, S. Tanaka, J. Dong, and B. P. Clayman: J. Phys. Condens. Matter **13** (2001) 5463.
- 11) Y. Nishio, Y. Nihei, M. Tamura, K. Kajita, T. Nakamura, and T. Takahashi: Synth. Met. **103** (1999) 1907.
- 12) H. Mori, T. Okano, S. Tanaka, M. Tamura, Y. Nishio, K. Kajita, and T. Mori: J. Phys. Soc. Jpn. **69** (2000) 1751.
- 13) M. Watanabe, Y. Nogami, K. Oshima, H. Mori, and S. Tanaka: J. Phys. Soc. Jpn. **68** (1999) 2654.
- 14) Y. Nogami, J. P. Pouget, M. Watanabe, K. Oshima, H. Mori, and S. Tanaka: Synth. Met. **103** (1999) 1911.
- 15) *For a review of nonlinear conductivity in organic crystals, see* T. Mori, I. Terasaki, and H. Mori: J. Mat. Chem. **17** (2007) 4343.
- 16) K. Inagaki, I. Terasaki, H. Mori, and T. Mori: J. Phys. Soc. Jpn. **73** (2004) 3364.
- 17) T. Yamaguchi, T. Konoike, K. Enomoto, M. Nishimura, T. Terashima, S. Uji, and H. M. Yamamoto: Phys. Rev. Lett. **96** (2006) 136602; *ibid* **98** (2007) 116602.
- 18) F. Sawano, I. Terasaki, H. Mori, T. Mori, M. Watanabe, N. Ikeda, Y. Nogami, Y. Noda: Nature **437** (2005) 04087.
- 19) *As a Review, see* H. Seo, J. Merino, H. Yoshikawa, and M. Ogata: J. Phys. Soc. Jpn. **75** (2006) 051009
- 20) H. Kino and H. Fukuyama: J. Phys. Soc. Jpn. **64** (1995) 1877; *ibid* **64** 2726; *ibid* **64** 4523; *ibid* **65** 2158.
- 21) H. Seo: J. Phys. Soc. Jpn. **69** (2000) 805.
- 22) T. Mori: J. Phys. Soc. Jpn. **72** (2003) 1469.
- 23) J. Merino, H. Seo, and M. Ogata: Phys. Rev. B **71** (2005) 125111.
- 24) M. Kaneko and M. Ogata: J. Phys. Soc. Jpn. **75** (2006) 014710.
- 25) H. Watanabe and M. Ogata: J. Phys. Soc. Jpn. **75** (2006) 063702.
- 26) L. P. Keldysh: Sov. Phys. JETP **20** (1965) 1018.
- 27) H. Haug and A. P. Jauho: *Quantum Kinetics in Transport and Optics of Semiconductors*, ed. H. K. V. Lotsch (Springer, Heidelberg, Germany, 1998) p. 95.